J Therm Anal Calorim (2009) 98:387–394
DOI 10.1007/s10973-009-0290-2

Synthesis, spectral and thermal properties of some transition metal(II) complexes with a novel ligand derived from thiobarbituric acid

Xiaoyi Li · Yiqun Wu · Donghong Gu · Fuxi Gan

Received: 16 September 2008 / Accepted: 13 January 2009 / Published online: 28 July 2009

Abstract Four novel metal(II) complexes, $Ni(L)_2$, $Co(L)_2$, $Cu(L)_2$, and $Zn(L)_2$ (L = 5-(2-(1,5-dimethyl-3-oxo-2-phenyl-2,3-dihydro-1H-pyrazol-4-yl)hydrazono)-1,3-diethyl-2-thioxo-dihydropyrimidine-4,6(1H,5H)-dione), were synthesized using the procedure of diazotization, coupling and metallization. Their structures were identified by elemental analyses, ^{1}H NMR, ESI-MS and FT-IR spectra. The effect of different central metal(II) ions on absorption bands of the metal(II) complexes was researched. The thermal properties of the metal(II) complexes were investigated by thermogravimetry (TG) and differential scanning calorimetry (DSC). Furthermore, the thermodynamic parameters, such as activation energy (E^*), enthalpy (ΔH^*), entropy (ΔS^*) and free energy of the decomposition (ΔG^*) are calculated from the TG curves applying Coats–Redfern method. The results show that the metal(II) complexes have suitable electronic absorption spectra with blue-violet light absorption at about 350–450 nm, high thermal stability with sharp thermal decomposition thresholds.

Keywords Thiobarbituric acid · Metal(II) complexes · Absorption spectra · Thermal property · Thermodynamic parameters

X. Li · Y. Wu (✉) · D. Gu · F. Gan
Key Laboratory of High Power Laser Materials, Shanghai Institute of Optics and Fine Mechanics, Chinese Academy of Sciences, No. 390, Qinghe Road, Jiading District, Shanghai 201800, People's Republic of China
e-mail: yqwu@siom.ac.cn

Y. Wu
Key Lab of Functional Inorganic Material Chemistry (Heilongjiang University), Ministry of Education, Haerbin 150080, People's Republic of China

Introduction

With the emerging of high-definition television broadcasting, the storage of over two-hour program has been required and a new high density optical storage disc format, which is called Blu-ray disc (BD), has been developed. BD system uses a 405 nm blue-violet laser and an objective lens with numerical aperture (NA) of 0.85 that can write small bits and thus increases the data storage capacity [1, 2]. Organic dyes, especially metallized organic dyes which are with modifiable molecular structures, low cost, and easy fabrication, have attracted much attention [3–5]. Recently, metal(II) complexes based on barbituric acid were found with interesting electronic and geometrical features in connection with their application in nonlinear optical elements, printing system, and this kind of compounds may be a potential medium for information storage [6–8]. As is known, the optical and thermal recording mechanism is governed by the changes of the optical properties of the recording material induced by the irreversible local thermal decomposition or thermal deformation, which are mainly depended on the absorption and thermal properties, etc. [4, 5], so understanding of the basic properties are important for a material used as a optical recording media. But little study has been done on these properties of transition metal complexes derived from thiobarbituric acid. In this work, four novel metal(II) complexes with blue-violet light absorption were synthesized by a new ligand from 1,3-diethyl-2-thiobarbituric acid and 4-aminoantipyrine reacting with transition metals (nicket(II), cobalt(II), copper(II) and zinc(II)) ions. The chemical structures of both the free ligand and its metal(II) complexes were studied. The effect of different central metal(II) ions on absorption bands of the metal(II) complexes was researched. Furthermore, the thermal properties

of the metal(II) complexes were investigated and the activation thermodynamic parameters, such as activation energy, enthalpy, entropy and free energy of the decomposition were calculated. All these properties imply that this kind of metal(II) complexes has a promising use in blu-ray disc-recordable systems for next generation optical storage.

Experimental

Materials

All the reagents and solvents in this work were of reagent-grade quality. 4-Aminoantipyrine and 1,3-diethyl-2-thiobarbituric acid were purchased from Sinopyarm Chemical Reagent Co., Ltd and Acros Chemical Co. respectively and used without further purification. A facile route was adopted in the synthesis of the ligand and its metal(II) complexes and the synthetic schemes together with suggested structures are shown in Fig. 1.

Synthesis of 5-(2-(1,5-dimethyl-3-oxo-2-phenyl-2,3-dihydro-1H-pyrazol-4-yl) hydrazono)-1,3-diethyl-2-thioxo-dihydropyrimidine-4,6(1H,5H)-dione ligand (HL)

Diazotization

4-Aminoantipyrine (4.0650 g, 0.020 mol) was dissolved in 40 mL concentrated phosphoric acid (85%) at room temperature. The solution was then cooled to −5 to 0 °C in an ice–salt bath and maintained at this temperature, solution of sodium nitrite (1.4861 g, 0.021 mol) in water (10 mL) was added dropwise within 1 h under continuous stirring and the mixture was stirred at 0–5 °C 1 h. The resulting diazonium solution was used directly in the coupling step.

Coupling

The coupling component (1,3-diethyl-2-thiobarbituric acid, 4.4055 g, 0.022 mol) was dissolved in 200 mL sodium hydroxide solution (2%, pH = 14) and cooled to −5 to 0 °C in an ice–salt bath. The above diazonium solution was added to the stirred coupling component solution at −5 to 0 °C over 30 min, maintaining the pH at 8–10. The mixture was allowed to rise to room temperature over 4 h and the pH was lowered to about 5. The precipitated solid was filtered with suction, washed with water and then vacuum dried. The rough product was finally purified by column chro matography to give 5-(2-(1,5-dimethyl-3-oxo-2-phenyl-2,3-dihydro-1H-pyrazol-4-yl)hydrazono)-1,3 -diethyl-2-thioxo-dihydropyrimidine-4,6(1H,5H)-dione ligand (HL).

General procedure for the synthesis of the metal(II) complexes

The resulting ligand (0.69 mmol) was dissolved in 40 mL of ethanol together with 0.691 mmol of sodium acetate. After heating up to reflux, the metal(II) acetate (0.35 mmol) dissolved in 2 mL water was added dropwise under vigorous stirring, whereupon a suspension of the metal(II) complex dye results. The precipitated solid was collected by filtration, washed with water and then vacuum dried to obtain the metal(II) complex.

Some physico-chemical and elemental analysis data of the synthesized ligand and its metal(II) complexes are given in Table 1.

Instrument and methods

The melting points of the compounds were determined using an XT-4 microscopic melting point apparatus (made in China) and were uncorrected. Elemental analyses of C, H and N were carried out on a Vario EL elemental

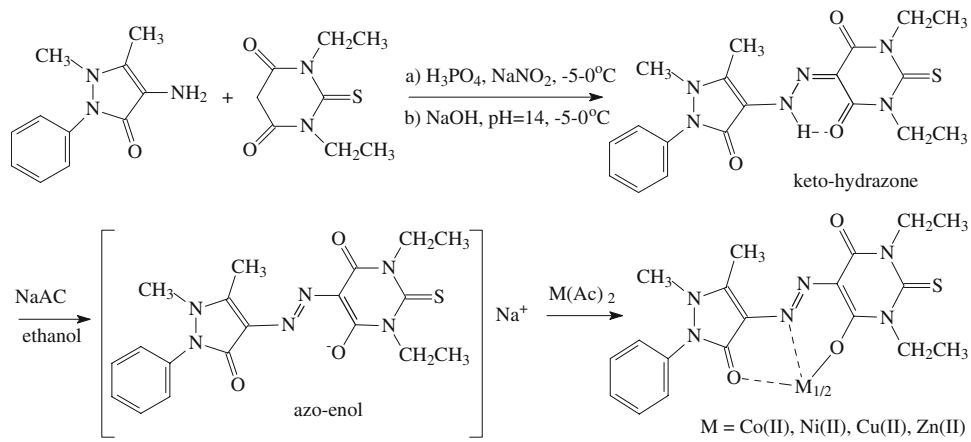

Fig. 1 Synthetic schemes of ligand and its metal(II) complexes

Table 1 Physico-chemical and elemental analysis data of the ligand and its metal(II) complexes

Compound (formula)	Yield/%	mp/°C	Calc. (found)/%			m/z Calc. (found)	λ_{max}/nm in chloroform
			C	H	N		
HL ($C_{19}H_{22}N_6O_3S$)	83	220–225	55.06 (54.98)	5.35 (5.29)	20.28 (20.04)	414.1 (415.1)$[M + H]^+$	461
$Co(L)_2$ ($C_{38}H_{42}N_{12}O_6S_2Co$)	64	>320	51.52 (51.46)	4.78 (4.70)	18.97 (18.91)	885.2 (886.2)$[M + H]^+$	432
$Ni(L)_2$ ($C_{38}H_{42}N_{12}O_6S_2Ni$)	71	>327	51.53 (51.49)	4.78 (4.69)	18.98 (18.92)	884.2 (885.2)$[M + H]^+$	435
$Cu(L)_2$ ($C_{38}H_{42}N_{12}O_6S_2Cu$)	45	>230	51.25 (51.13)	4.75 (4.67)	18.87 (18.91)	889.2 890.1$[M + H]^+$	443
$Zn(L)_2$ ($C_{38}H_{42}N_{12}O_6S_2Zn$)	59	>300	51.15 (51.09)	4.74 (4.69)	18.84 (18.68)	890.2 (891.2)$[M + H]^+$	441

analyzer. FT-IR spectra were obtained in KBr pellets on a Perkin-Elmer FT-IR 1650 spectrometer in the 4000–400 cm^{-1} region. ^1H NMR spectra (DMSO solutions) were recorded on a Brucker 400 MHz Spectrometer in DMSO-d_6 using TMS as an internal reference. ESI mass spectra were performed using a Surveyor LCQ spectrometer. UV–vis spectra were measured using a Perkin-Elmer Lambda 9UV/VIS/NIR spectrophotometer. Thermal properties were analyzed with a TA instrument, the SDT Q600 Simultaneous DSC/TG Analyzer, at a heating rate of 10 °C min^{-1} from 50 to 700 °C under nitrogen atmosphere, using 2–6 mg of powdered samples in a nitrogen atmosphere.

Results and discussion

Synthesis and characterization

The ligand was synthesized by diazo coupling reaction. It may exist in keto-hydrazone and azo-enol tautomeric forms as shown in Fig. 1. It has been shown, conclusively from a series of investigations using various techniques, such as IR, NMR and X-ray crystallography, that hydrazones containing 4,6-dicarbonyl groups exist exclusively in the keto-hydrazone form both in solution and in the solid state [9–12]. An intramolecular hydrogen bridge linking one of the carbonyl groups to the NH-moiety of the hydrazone unit was found to be a characteristic feature of this compound class. The six-membered intramolecular hydrogen bonding ring is possible in the keto-hydrazone tautomer as showed in Fig. 1. The infrared spectra of hydrazone based on a substituted 4,6-dione and, in particular the position of the carbonyl stretching vibrations, have been of considerable importance in establishing that the compounds exist exclusively in the keto-hydrazone form. The solid state IR spectra of the synthesized ligand shows three intense carbonyl bands (1689 (νC=O···H), 1660 (νC=O), 1629 (νC=O) cm^{-1}) consistent with a keto-hydrazone form. It can be suggested that the ligand exists as keto-hydrazone form with extensive six-membered intramolecular hydrogen bonding, and this has been confirmed by a number of previous published reports of keto-hydrazone analogues [10, 12, 13]. Another typical feature of the free ligand is the existence of an NH vibration around 3100 cm^{-1} which affords proof of the H-bonded hydrazone structure in the solid state also [9, 14]; the remaining vibrational frequencies obtained and their tentative assignments are shown in Table 2. In the ^1H NMR spectra of the ligand measured in DMSO-d_6, the hydrazone proton appears as a singlet at 14.5 ppm, which corresponds to imine NH proton resonance of the hydrazone form. Furthermore, the ^1H NMR spectra of some dyes reported in DMSO-d_6 exist in the hydrazone form and show NH peaks within the range of 13.50–15.10 ppm [15–17]. The ^1H NMR other spectra of the ligand show a singlet at 3.27 ppm (N–CH_3 of antipyrine ring), a singlet at 2.48 ppm (C–CH_3 of antipyrine ring), a triplet at 1.17–1.21 ppm (CH_3 of thiobarbituric acid ring), a quartet at 4.06–4.42 ppm (CH_2 of thiobarbituric acid ring), multi signals at 7.39–7.54 ppm (CH of pheny). The above results suggest that the ligand prepared exists in the keto-hydrazone form in the solid state, and the obtained IR spectra, ESI mass spectra, ^1H NMR and elemental analytical data agree well with the formulae of the ligand.

Table 2 Significant FT-IR bands and tentative assignments of the ligand and its metal(II) complexes

Compound	νH–N (hydrazone)	νAro–H	νAl–H	νC=O	νN=N	νC–O(enol hydroxyl)	νM–N	νM–O
HL	3100	3020	2868–2977	1689, 1660, 1629	–	–	–	–
$Co(L)_2$	–	3053	2872–2976	1662, 1603	1414	1264	454	509
$Ni(L)_2$	–	3056	2872–2977	1664, 1606	1415	1263	461	509
$Cu(L)_2$	–	3059	2871–2976	1653, 1602	1417	1265	474	508
$Zn(L)_2$	–	3048	2868–2977	1652, 1603	1415	1262	448	505

The metal(II) complexes were synthesized by reaction of the relevant metal(II) acetate with the ligand. Due to the possible keto-hydrazone and azo-enol tautomerism of the prepared ligand [11], the action of the sodium acetate on the ligand in solution is to convert the keto-hydrazone form into the azoanion form [18, 19]. Consequently, metal(II) complexes were easily synthesized by the chelation of the metal(II) ion and ligand in the azo-enol form (see Fig. 1). The elemental analytical data, ESI mass spectra and FT-IR spectra of the metal(II) complexes agree well with their formulae. The metal-to-ligand ratios of the four metal(II) complexes were found to be 1:2. Figure 1 shows the suggested structure of the metal(II) complexes.

FT-IR spectra of the ligand and its metal(II) complexes

The important IR characteristic absorption bands, along with their proposed assignments, are summarized in Table 2. As seen from Table 2, the IR spectra of the metal(II) complexes were similar to each other, except for some slight shifts and intensity changes of a few vibration bands caused by different metal(II) ions, which indicates that the complexes were of similar structure. However, there were some significant differences between the free ligand and the metal(II) complexes. The coordination mode and sites of the ligand to the metal(II) ions were investigated by comparing the infrared spectra of the free ligand with its metal(II) complexes. Upon coordination, it is noteworthy that two strong absorption bands in the region 1602–1664 cm^{-1} attributed to νC=O vibration were shifted by 20–30 cm^{-1} on complexation, while the third carbonyl absorption band at 1689 cm^{-1}, appearing in the spectra of the free ligand with the extensive six-membered intramolecular hydrogen bonded structure, was not observed. These results indicate that the ligand are in the azo-enol form in the complex which naturally forms an enolic hydroxyl oxygen and an enolic carbony with consequent replacement of the enolic hydrogen by the metal(II) ion [3]. A new band due to C–O vibration appearing at 1262–1265 cm^{-1} in the spectra of all the metal(II) complexes can be further evidence for the bonding of the enol hydroxyl oxygen to the metal(II) ion [9, 11, 20]. Furthermore, the medium-intensity band at 3100 cm^{-1} of the free ligand, due to νNH stretching, disappears in the complexes, suggesting that the NH proton is lost via enolization and the resulting enolic oxygen and azoic nitrogen take part in coordination [5, 9]. Moreover, another new band due to –N=N– vibration appears around 1414–1417 cm^{-1} in the spectra of all the complexes, which supports the azo-enol form of the ligand in the metal(II) complexes; the appearance of this peak at relatively lower field may indicate coordination via the N=N group [3, 21]. In addition, the IR spectrum of the ligand reveals a sharp band at about 1629 cm^{-1} corresponding to the νC=O of the antipyrine ring, which was shifted to a lower frequency by about 20–30 cm^{-1} after complexation in all metal(II) complexes, suggesting that the oxygen atom of the antipyrine ring also contributes to complexation [20, 22]. The mode of bonding of the metal(II) ion is further supported by the broad absorption bands in the region 505–509 and 448–474 cm^{-1}, which can be assigned to νM–O and νM–N stretching vibrations, respectively [22–25]. Therefore, from these IR spectra, it is concluded that the ligand may exist in azo-enol form during complexation and behave as a O,N,O′-monobasic tridentate ligand coordinated to metal(II) ions via the enolic hydroxyl O, azoic group N and O of the antipyrine ring.

UV–vis electronic absorption spectra of the ligand and its metal(II) complexes

Figure 2 gives the electronic absorption spectra of the ligand and its metal(II) complexes in $CHCl_3$ solutions. It can be seen that the ligand has three absorption bands. The first one appearing below 250 nm may be attributed to $\pi \rightarrow \pi^*$ transition of the heterocyclic moiety and/or phenyl ring. The second band observed at 330 nm is attributed to $\pi \rightarrow \pi^*$ transition of the C=O groups [20]. The third band appearing around 461 nm can be assigned to $n \rightarrow \pi^*$ transition involving the whole electron system of the ligand [22]. In the spectra of the metal(II) complexes, their absorption bands are hypsochromically shifted comparative to the corresponding bands of the free ligand. The results in our experiments can be explained as follows: the visible absorption band of the ligand as the azoanion form are observed a hypsochromically shift comparative to that of the hydrazone ligand [19, 26]. The above effects in visible spectra of the metal(II) complexes may support the

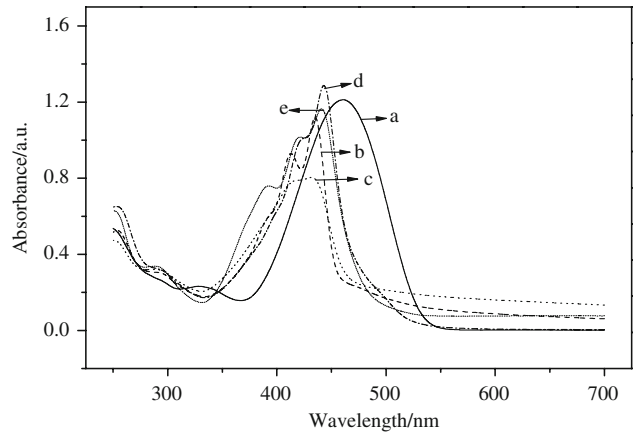

Fig. 2 Absorption spectra of the ligand and its metal(II) complexes in chloroform: (a) ligand (HL); (b) $Ni(L)_2$; (c) $Co(L)_2$; (d) $Cu(L)_2$; (e) $Zn(L)_2$

participation as anion of the ligand. Otherwise this assumption is very reasonable [18, 27, 28].

From Fig. 2, it also can be observed that the maximal absorption peak of the free ligand is at 461 nm, but those of its metal(II) complexes are at 432, 435, 443 and 441 nm for $Co(L)_2$, $Ni(L)_2$, $Cu(L)_2$ and $Zn(L)_2$, and blue shift 29, 26, 18 and 20 nm comparative to the free ligand, respectively. This also indicates that center metals have influence on the absorption bands of the complexes. According to modern molecular orbital theory [26], any factor, such as the electronegativity, the radius and electronic configuration of the metal(II) ion, that can influence the electronic density of a conjugated system must result in the difference of the absorption band. For metal(II) ions, in generally, the ability to attract the electron enhances with the electronegativity increasing and the radii reducing. In the complexes $Co(L)_2$, $Ni(L)_2$, $Cu(L)_2$, the order of electronegativity metal(II) ions is 1.88 $Co^{2+}(d^7) < 1.91$ $Ni^{2+}(d^8) < 2.0$ $Cu^{2+}(d^9)$, the order of radii is Co^{2+} (0.74 Å) > Ni^{2+} (0.72 Å) > Cu^{2+} (0.69 Å), so the ability to attract the electrons from the oxygen and nitrogen should be Co(II) < Ni(II) < Cu(II), and the n electronic density in the conjugated system is increased from $Co(L)_2$ to $Cu(L)_2$, and the energy gaps of $n \rightarrow \pi^*$ is reduced from $Co(L)_2$ to $Cu(L)_2$, Therefore, the blue shift is $Co(L)_2 > Ni(L)_2 > Cu(L)_2$, which is well in agreement with our experiment results. Except for $Zn(L)_2$, because of its fully filled d-orbit (d^{10}). Furthermore, from the Fig. 2 it can be found that these complexes have suitable absorption at 405 nm, and could well matched with blue laser. These characteristics imply that these complexes may have potential application for blu-ray optical storage.

Thermal properties of the metal(II) complexes

The thermal properties of the metal(II) complexes were investigated by thermogravimetric (TG) analysis, differential thermogravimetric (DTG) and differential scanning calorimetry (DSC). Figure 3 presents the recorded TG/DTG and DSC curves of four metal(II) complexes in nitrogen atmosphere. It can be seen that the TG curves of the complexes show no any mass loss up to 200 °C, indicating the absence of water molecule and any other adsorptive solvent molecules in the coordination sphere. As the temperature is increased, the TG/DTG curves of the four metal(II) complexes exhibit a sharp mass loss at temperature of about 240–340 °C, which are accompanied with a sharp exothermic peak in the DSC curves. The correlations between the different decomposition steps of the metal(II) complexes with the corresponding mass losses are discussed in terms of the proposed formulae of the metal(II) complexes.

The $Ni(L)_2$ complex shows only one-step decomposition. This step shows drastic mass loss of 47.89% within a wide

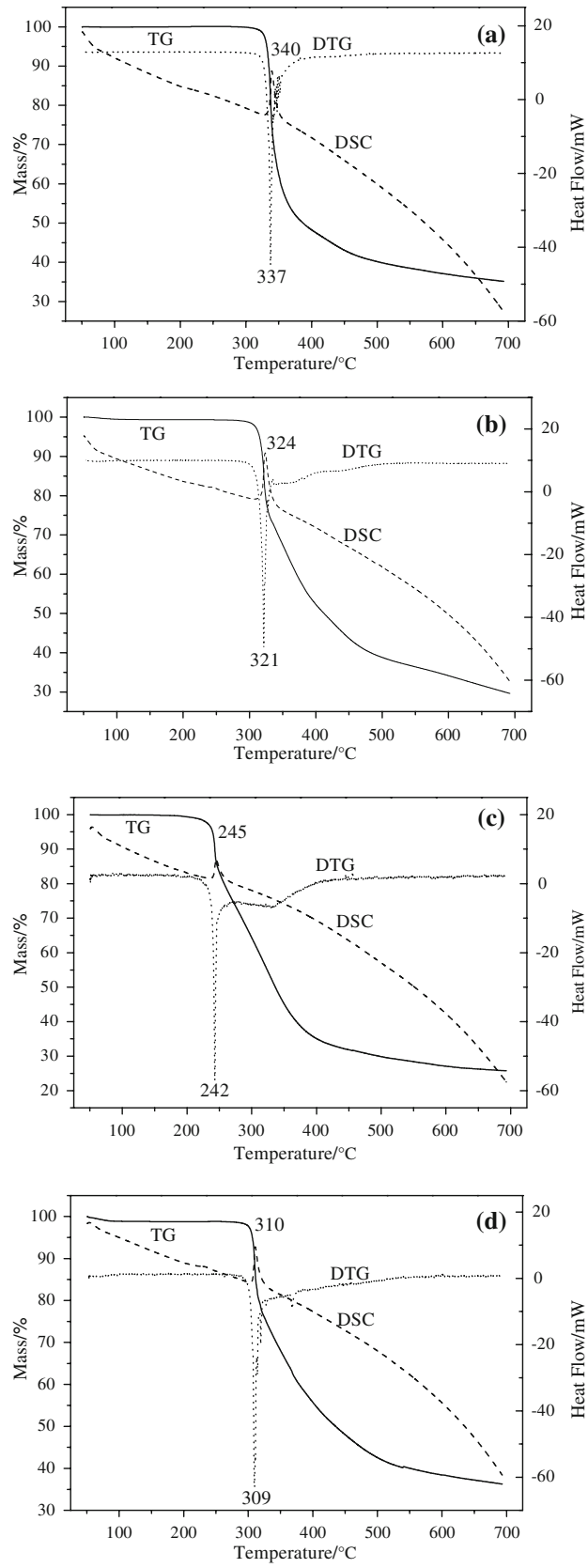

Fig. 3 TG/DTG and DSC curves of the metal(II) complexes: **a** $Ni(L)_2$; **b** $Co(L)_2$; **c** $Cu(L)_2$; d $Zn(L)_2$

temperature range 319–375 °C with the DTG peak at 337 °C, also giving rise to a sharp exothermic peak at 340 °C in DSC curve. This process can be readily interpreted as loss of one ligand molecule ($Ni(L)_2 \rightarrow Ni(L) + L$) (calcd. 46.69%). The following decomposition of the $Ni(L)_2$ complex exhibits a gradual mass loss process in the rest of temperature range, and shows no obvious peaks both in the DTG and DSC curves.

The $Co(L)_2$ complex is thermally decomposed in two successive decomposition steps within the temperature range 50–700 °C. The first decomposition step of estimated mass loss 26.70% within the temperature range 305–334 °C may be attributed to the loss of the $C_{11}H_{11}N_4O$ molecule (diazo part of the ligand) (calcd. 24.40%). Simultaneously, the DTG peak corresponding to this stage is observed at 321 °C. The recorded DSC curve reveals sharp exothermic peak at 324 °C. The second step occurs with the temperature range 336–700 °C, which may be accounted for the decomposition of the remaining ligand molecules, and shows no obvious peaks in DSC curve.

The $Cu(L)_2$ complex is thermally decomposed in two successive decomposition steps. The first decomposition step of estimated mass loss 25.78% within the temperature range 219–272 °C may be attributed to the loss of the $C_{11}H_{11}N_4O$ molecule (calcd. 24.27%). The DTG peak corresponding to this stage is observed at 242 °C. The recorded DSC curve reveals sharp exothermic peak at 245 °C. The second step occurs with the temperature range 272–700 °C with a DTG peak at 335 °C, which may be due to the decomposition of the remaining ligand molecules, and shows no obvious peaks in DSC curve.

The $Zn(L)_2$ complex shows decomposition pattern of two stages. The first step displays a sharp mass loss of 24.67% within the temperature range 290–326 °C with a DTG peak at 309 °C, which may be attributed to the loss of the $C_{11}H_{11}N_4O$ molecule (calcd. 24.12%). The recorded DSC curve reveals sharp exothermic peak at 310 °C. After the rapid mass loss of the $Zn(L)_2$ complexes, the second step exhibits a gradual loss in mass within the remaining temperature range with a DTG peak at 369 °C, which may be attributed to the decomposition of the remaining ligand molecules. This step shows no obvious peaks in DSC curve.

The above TG and DTG data reveal that the decomposition pattern is different. The $Ni(L)_2$ complex exhibits only one-step decomposition, whereas a two-stage decomposition is observed in the case of $Co(L)_2$, $Cu(L)_2$ and $Zn(L)_2$ complexes. According to the beginning temperature of the decomposition of the metal(II) complexes the following order of thermal stability may be proposed: $Ni(L)_2 > Co(L)_2 > Zn(L)_2 > Cu(L)_2$. The difference in thermal stability of the metal(II) complexes reveals that the metal(II) ion may have some marked influence on the thermal stability.

Kinetic studies of non-isothermal decomposition

The kinetic parameters of the first decomposition process of the metal(II) complexes were calculated from the non-isothermal TG curves, with heating rate of 10 °C min^{-1}, using Coats–Redfern method [29]. The equations are used in the forms:

$$\ln\left[\frac{1-(1-\alpha)^{1-n}}{T^2(1-n)}\right] = \ln\left[\frac{AR}{\beta E^*}\left(1-\frac{2RT}{E^*}\right)\right] - \frac{E^*}{RT} (n \neq 1) \quad (1)$$

$$\ln\left[\frac{-\ln(1-\alpha)}{T^2}\right] = \frac{-E^*}{RT} + \ln\left[\frac{AR}{\beta E^*}\right] (n = 1). \quad (2)$$

Where α is the fraction of sample decomposed at temperature T, R is the gas constant, A is the pre-exponential factor, n is reaction order, E^* is the activation energy in kJ mol^{-1}, β is the heating rate and $(1 - (2RT/E^*) \cong 1$.

Plots of $\ln\{[1-(1-\alpha)^{1-n}]/[T^2(1-n)]\}$ against $1/T$ for different values of n have been tested and $\ln[-\ln(1-\alpha)/T^2]$ against $1/T$ has also been tested. The correct value of n for the thermal reaction is the one which gives the best straight line (shown in Fig. 4). From the slope of the straight line the activation energy E^* could be calculated, where the slope $= -E^*/R$. A was determined from the intercept. The entropy of activation (ΔS^*), enthalpy of activation (ΔH^*) and the free energy change of activation (ΔG^*) were calculated using the following equations:

$$\Delta S^* = 2.303R \log\left(\frac{Ah}{kT_s}\right) \quad (3)$$

$$\Delta H^* = E^* - RT_S \quad (4)$$

$$\Delta G^* = \Delta H^* - T_S \Delta S^* \quad (5)$$

where k, h and T_s are the Boltzman constant, Planck constant and the DTG peak temperature, respectively.

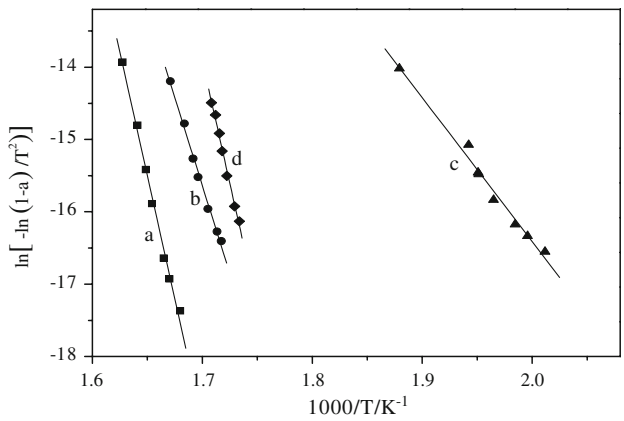

Fig. 4 Coats and Redfern plots for the metal(II) complexes: (a) $Ni(L)_2$; (b) $Co(L)_2$; (**c**) $Cu(L)_2$; (d) $Zn(L)_2$

Table 3 The thermal behavior and kinetic parameters of the metal (II) complexes

Complex	Temperature range/°C	Mass loss found (calc.)/%	E^*/kJ mol^{-1}	A/s^{-1}	ΔS^*/J K^{-1} mol^{-1}	ΔH^*/kJ mol^{-1}	ΔG^*/kJ mol^{-1}
$Ni(L)_2$	319–375	47.89 (46.69)	565.35	3.89×10^{44}	602.85	560.28	192.45
$Co(L)_2$	305–334	26.70 (24.30)	404.39	3.02×10^{31}	352.07	399.45	190.27
$Cu(L)_2$	221–272	25.48(24.18)	165.45	1.35×10^{12}	−17.23	161.16	170.04
$Zn(L)_2$	290–326	24.67 (24.12)	563.68	2.34×10^{46}	636.91	558.61	170.00

The activation energies of the metal(II) complexes were calculated from the Fig. 4. The calculated values of E^*, A, ΔS^*, ΔH^* and ΔG^* for the first decomposition step are given in Table 3. The kinetic parameters, especially activation energy E^* and activation entropy ΔS^* are helpful in assigning the strength of the bonding of ligand moieties with the metal ions. The activation energies of the first stage of decomposition for all the metal(II) complexes are in the range of 165.45–565.35 kJ mol^{-1}, which indicates bonding degree of ligand bound to metal ion. It was found that the order of the activation energy values of the different metal(II) complexes is $Ni(L)_2 > Zn(L)_2 > Co(L)_2 > Cu(L)_2$. This difference may be due to the stereostructure of the metal(II) complexes and electronic configuration of the metal(II) ion. The ΔS^* values of the first stage for all the metal(II) complexes were found to be positive except for the $Cu(L)_2$ complex, indicating that the activated complexes were less ordered than the reactants [30].

Conclusions

In conclusion, we described the synthesis and some spectroscopic and thermal properties of the ligand derived from thiobarbituric acid and its four transition metal(II) complexes. The possible structures of the ligand and its metal(II) complexes were proposed and the thermal properties of the metal complexes were investigated as well. The various thermodynamic activation parameters (E^*, ΔH^*, ΔS^* and ΔG^*) were calculated. It was found that these metal(II) complexes show suitable electronic absorption spectra with blue-violet light absorption at about 350–450 nm, high thermal stability and sharp thermal decomposition threshold with high mass loss rate. These characteristics imply that these new complexes may be good candidates of optical recording media for blu-ray optical information storage.

Acknowledgements Financial support from the National Natural Science Foundation of China (No. 60490290), Chinese Academy of Sciences (KJCX2.YW.M06) and the National Science and Technology Program of China (No. 2007AA03Z412) is gratefully acknowledged.

References

1. Kuwahara M, Takehara S, Kashihara Y, Watabe K, Nakano T, Tanaka M, et al. Experimental study of high-density rewritable optical disk using a blue-laser diode. Jpn J Appl Phys. 2003;42:1068–71.
2. Chang D, Yoon D, Ro M, Park I, Shin D. Synthesis and characteristics of protective coating on thin cover layer for high density-digital versatile disc. Jpn J Appl Phys. 2003;42:754–8.
3. Huang FX, Wu YQ, Gu DH, Gan FX. Spectroscopic and thermal properties of short wavelength metal (II) complexes containing α-isoxazolylazo-β-diketones as co-ligands. Spectrochim Acta A. 2005; 61:2856–60.
4. Park H, Kim ER, Kim DJ, Lee H. Synthesis of metal-azo dyes and their optical and thermal properties as recording materials for DVD-R. Bull Chem Soc Jpn. 2002;75:2067–70.
5. Chen ZM, Wu YQ, Gu DH, Gan FX. Nickel(II) and copper(II) complexes containing 2-(2-(5-substitued isoxazol-3-yl)hydrazono)-5,5-dimethylcyclohexane- 1,3-dione ligands: synthesis, spectral and thermal characterizations. Dye Pigment. 2008;76: 624–31.
6. Wang S, Shen S, Xu H. Synthesis, spectroscopic and thermal properties of a series of azo metal chelate dyes. Dye Pigment. 2000;44:195–8.
7. Wu SJ, Qian W, Xia ZJ, Zou YH, Wang SQ, Shen SY, et al. Investigation of third-order nonlinearity of an azo dye and its metal-substituted compounds. Chem Phys Lett. 2000;330:535–40.
8. Abe T, Mano S, Yamada Y, Tomotake A. Thermal dye transfer printing with chelate compounds. J Imaging Sci Technol. 1999;43:339–44.
9. Gup R, Gizioglu E, Kırkan B. Synthesis and spectroscopic properties of new azo-dyes and azo-metal complexes derived from barbituric acid and aminoquinoline. Dye Pigment. 2007;73:40–6.
10. Karcı F, Karcı F. The synthesis and solvatochromic properties of some novel heterocyclic disazo dyes derived from barbituric acid. Dye Pigment. 2008;77:451–6.
11. Song HF, Chen KC, Tian H. Synthesis of novel dyes derived from 1-ethyl-3-cyano-6-hydroxy-4-methyl-5-amino-2-pyridone. Dye Pigment. 2002;53:257–62.
12. Kirkan B, Gup R. Synthesis of new azo dyes and Copper(II) complexes derived from barbituric acid and 4-aminobenzoylhydrazone. Turk J Chem. 2008;32:9–17.
13. Christie RM, Dryburgh WT, Standring PN. Some monoazo-acetoacetanilide pigments derived from heterocyclic diazo components. Dye Pigment. 1991;16:231–40.
14. El-Boraey HA, El-Saied FA, Aly SA. UO_2(VI), Sn(IV), Th(IV) and Li(I) complexes of 4-azomalononitrile antipyrine. J Therm Anal Calorim 2009;96:599–606. doi:10.1007/s10973-008-9197-6.
15. Karcı F, Karcı F. Synthesis and absorption spectra of some novel heterocyclic disazo dyes derived from pyridone and pyrazolone derivatives. Dye Pigment. 2008;76:147–57.

16. Ertan N, Gürkan P. Synthesis and properties of some azo pyridone dyes and their Cu(II) complexes. Dye Pigment. 1997;33: 137–47.
17. Peng Q, Li M, Gao K, Cheng L. Hydrazone-azo tautomerism of pyridone azo dyes: Part 1—NMR Spectra of Tautomers. Dye Pigment. 1990;14:89–99.
18. Bâtiu C, Panea I, Ghizdavu L, David L, Ghizdavu Pellascio S. Divalent transition metal complexes 4-(4-ethoxy-phenylhydrazono)-1-phenyl-3-methyl-1H-pyrazolin-5 (4H)-one. J Therm Anal Calorim. 2005;79:129–34.
19. Peng Q, Li M, Gao K, Cheng L. Hydrazone-azo tautomerism of pyridone azo dyes: Part III—effect of dye structure and solvents on the dissociation of pyridone azo dyes. Dye Pigment. 1992;18: 271–86.
20. Issa RM, Khedr AM, Rizk HF. UV–vis, IR and ^{1}H NMR spectroscopic studies of some Schiff bases derivatives of 4-aminoantipyrine. Spectrochim Acta A. 2005;62:621–9.
21. Ropret P, Centeno SA, Bukovec P. Raman identification of yellow synthetic organic pigments in modern and contemporary paintings: reference spectra and case studies. Spectrochim Acta A. 2008;69: 486–97.
22. Abdel-Latif SA, Hassib HB. Studies of Mn(II), Co(II), Ni(II) and Cu(II) Chelates with 3-phenyl-4-(p-methoxy-phenylazo)-5-pyrazolone. J Therm Anal Calorim. 2002;68:983–95.
23. Garg BS, Sharma RK, Kundra E. Copper(II), nickel(II), cobalt(II) and zinc(II) complexes of 2-[2-(6-methylbenzothiazolyl)azo]-5-dimethylaminobenzoic acid: synthesis, spectral, thermal and molecular modelling studies. Transition Met Chem. 2005;30: 552–9.
24. Omar MM, Mohamed GG. Potentiometric, spectroscopic and thermal studies on the metal chelates of 1-(2-thiazolylazo)-2-naphthalenol. Spectrochim Acta A. 2005;61:929–36.
25. Xu G-C, Zhang L, Liu L, Liu G-F, Jia D-Z. Kinetics of thermal decomposition of mixed-ligand nikkel(II) and copper(II) complexes of 4-acyl pyrazolone derivative and pyridine. J Therm Anal Calorim. 2007;89:547–53.
26. Griffiths J, Translated by Hou YF, Wu ZW, Hu JZ. Colour and constitution of organic molecules. Beijing: Chemistry Industry Press; 1985. p. 202.
27. Snavely FA, Suydam FH. Notes- structure of aryl azo pyrozolone compounds and their copper derivatives. J Org Chem. 1959;24: 2039–40.
28. Zaitev BE, Zaiteva VA, Molodkin AK, Obraztova ES. Synthesis and the structure of 1-phenyl-3-methyl-4-phenylazopyrazol-5-one with Cu(II) and Co(II). Zh Neorg Khim. 1979;24:127–33.
29. Coat AW, Redfern JP. Kinetic parameters from thermogravimetric data. Nature. 1964;201:68–9.
30. Kandil SS, El-Hefnawy GB, Baker EA. Thermal and spectral studies of 5-(phenylazo)-2-thiohydantoin and 5-(2-hydroxyphenylazo)-2-thiohydantoin complexes of cobalt(II), nickel(II) and copper(II). Thermochim Acta. 2004;414:105–13.